

**AN ANALYSIS OF RADIATION INDUCED STRESS IN GLASS AND CERAMICS
AS HIGH LEVEL WASTE FORMS**

T. M. Ahn and K. J. Swyler

**Department of Nuclear Energy
Brookhaven National Laboratory
Upton, New York 11973**

* Currently T. M. Ahn is at
U.S. Nuclear Regulatory Commission, Washington, DC 20555-0001

ABSTRACT

Glassy waste forms are often partially devitrified with dispersed small size crystalline phases, and crystalline waste forms consist of multiple phases. Also the radionuclides are inhomogeneously distributed within the waste form. Under these conditions, differential stresses can arise at interfaces and the concomitant microcracking would be expected to enhance leachability. In this work, we tabulate the data for radiation induced volume change in microcracking. To explain this phenomenon, radiation induced stresses and surface area increase are estimated with a first order approximation. For the stress calculation, we employ the stress distribution in a sphere, in a shell, or in a hollowed cylinder as determined from the linear isotropic elasticity theory. The calculations ^{are} ~~is~~ to assess stress from the difference of elastic moduli, stress from the differential swelling among phases and stress relaxation. The calculated stresses can cause microfracturing in agreement with experimental results and microfracture could increase surface area to a point where leaching behavior is significantly affected. The present calculation method can be extended to estimate radiation induced stresses from multibarrier waste forms.

ACKNOWLEDGMENT

This work was performed under the auspices of U. S. Nuclear Regulatory Commission. ~~The~~ authors acknowledge Dr. W. J. Weber of PNL for providing them their experimental results of glass cracking and Dr. D. M. Martin of Iowa State University for many helpful suggestions. ✓

Introduction

Solidified high level radioactive waste (HLW) forms will receive massive doses of self irradiation during their projected service life. Irradiation at the levels anticipated in HLW forms is known to cause measurable density changes in waste form materials: ceramics swell under irradiation, while glasses may either swell or compact. In certain cases, these changes may be accompanied by the formation of voids or (helium) gas-filled inclusions. Dimensional changes of this sort, if uncompensated for in package design, might produce unacceptably high stress levels in various parts of the waste package. Three cases are of particular interest: Many radionuclide (RN) host phases in HLW forms are microstructurally inhomogeneous; glassy waste forms are often partially devitrified with dispersed small size (1 to 1000 μm) crystalline phases; crystalline waste forms consist of multiple phases or polyphase crystalline structures. In either case the radionuclides may be inhomogeneously distributed within the waste form, resulting in an inhomogeneous radiation dose. Under these conditions, differential stresses can arise at interfaces or grain boundaries either from uniform swelling due to differences in elastic constants including anisotropy (Case I) or from nonuniform swelling or compaction in different phases (Case II). For either case, concomitant microcracking would be expected to enhance leachability. Finally, even a uniform volume change in the RN host phase, without cracking (Case III), would generate differential stresses in inert barrier components. Such components include waste containers, inert glass or PyC coatings, etc.

The practical consequences of radiation induced stresses in HLW packages do not seem to have been widely investigated; in fact, we are aware of only one intensive study. In this document we carry out a scoping analysis to identify those cases (if any) where more detailed consideration may be warranted. We begin by describing the relevant experimental data. This provides a basis for an estimation of anticipated stress levels and their practical implications.

Irradiation Induced Density Changes

Silicate glasses may either expand or compact under irradiation. The effect is illustrated for a number of different glasses¹ in Figure 1.

Zinc borosilicate waste glasses (72-68) compact under irradiation in both amorphous and devitrified form; the effect appears to saturate with alpha-dose at a volume contraction of about 1%. Both lead silicate and European borosilicate (high silica) waste glasses swell due to internal alpha decay. Weber, et al.,² have studied the stability of 77-260 glasses doped with curium. An overall swelling of about 1% was observed for the devitrified glass at a mean dose of 5×10^{18} alpha decays/cm³.

Radiation also causes ceramics to swell³; refractory oxides such as Al₂O₃ are known to exhibit swelling. Recently, neutron irradiation damage measurements have been reported for synthetic barium hollandite, perovskite, and un-

doped SYNROC B⁴. Samples were irradiated at 75-100°C to a dose considered equivalent to 2.2×10^{18} alphas/g and the results are shown in Table 1.

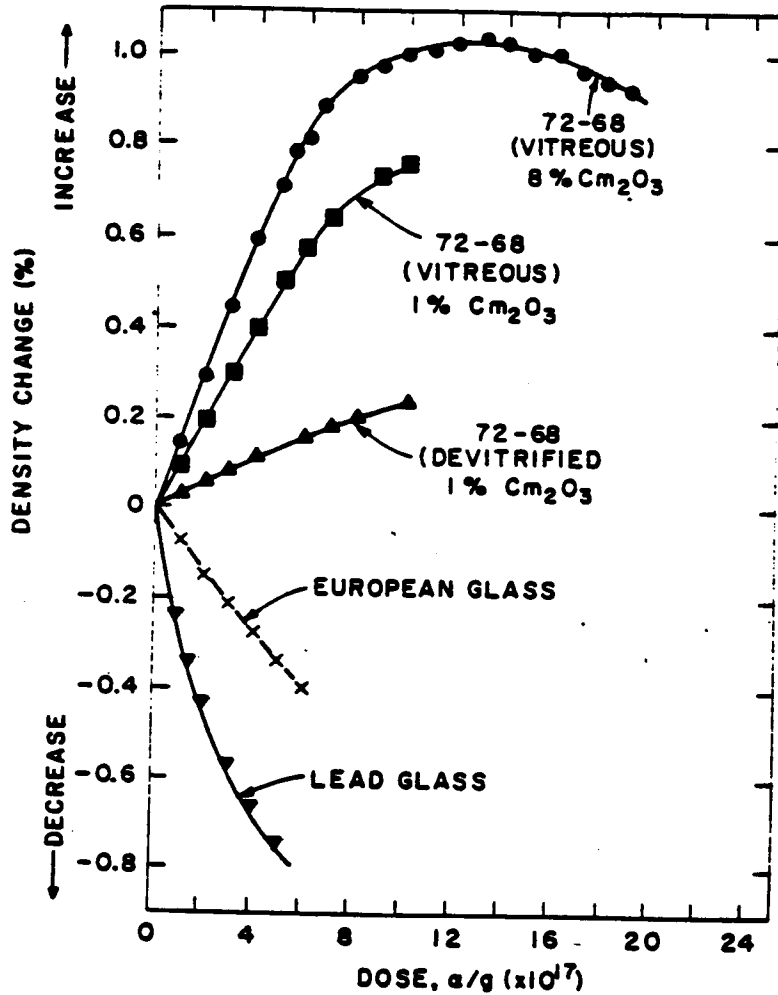


Figure 1. Density changes in glass doped with alpha emitters. From Mendel, et al.¹

Table 1. Average volume change (%) in irradiated SYNROC B and SYNROC C minerals.³

<u>SYNROC B</u>	<u>PEROVSKITE</u>	<u>HOLLANDITE</u>
1.68	2.64	1.44

Weber, et al.⁵ have extended their experiment of displacement damage by alpha particles and recoil nuclei to ceramics such as supercalcine, as well as to the crystalline phase in partially devitrified glass. Table 2 shows the maximum volume expansion in simulated waste forms, while Table 3 and Figure 2 represent the volume change to crystalline phase. It is noteworthy that the crystalline phase expand more (maximum 6%) than the glassy phase. They also have found that the volume changes saturate exponentially as dose increases.

Table 2. Crystalline materials studied at PNL by actinide doping and the maximum volume expansion observed.⁵

Material	Swelling $\Delta V/V$ (%)	Dose (α -decays/cm ³)
<u>Simulated Waste Forms</u>		
Partially Devitrified Glass ^a	1.0	5 x 10 ^{18e}
Celsian Glass Ceramic ^b	0.5	3 x 10 ^{18e}
Supercalcine, SPC-2 ^c	1.4	5 x 10 ^{18e}
Portland Cement, Type II ^d	<0.1	5 x 10 ¹⁷

^aPNL-77-260 waste glass, cooled at 6 K/h (Weber et al., 1979).²

^bStudied in cooperation with the Hahn-Meitner Institute (Berlin, West Germany).

^cRusin, Gray, and Wald (1979).⁶

^dContains 10 wt% simulated PW-9 calcine.

^eDose at saturation.

Table 3. Crystalline phases observed to become X-ray amorphous.⁵

<u>Parent Solid Form</u>	<u>Crystalline Phase</u>	<u>Volume Change To Crystalline Phase (%)</u>	<u>Amorphization Dose^e (α-decays/cm³)</u>
Partially Devitrified Glass	$\text{Ca}_3\text{Gd}_7(\text{SiO}_4)_5(\text{PO}_4)\text{O}_2^{\text{a}}$	3 ^c	1.5×10^{18}
Partially Devitrified Glass	$\text{Gd}_2\text{Ti}_2\text{O}_7^{\text{b}}$	Not Measurable	$>5 \times 10^{18}$
Celsian Glass Ceramic	$\text{Gd}_2\text{Ti}_2\text{O}_7^{\text{b}}$	1 ^c	3.2×10^{18}
Supercalcine SPC-2	$\text{Ca}_2\text{Nd}_8(\text{SiO}_4)_6\text{O}_2^{\text{a}}$	4 ^c	4.2×10^{18}
Pure compound	$\text{Ca}_2\text{Nd}_8(\text{SiO}_4)_6\text{O}_2^{\text{a}}$	$>6^{\text{d}}$	$>6 \times 10^{18\text{f}}$

^aApatite structure type.

^bPyrochlore structure type.

^cDetermined from XRD measurements.

^dDetermined from density measurements.

^eVolume averaged dose to complete sample.

^fThis compound has not yet reached a complete x-ray amorphous state.

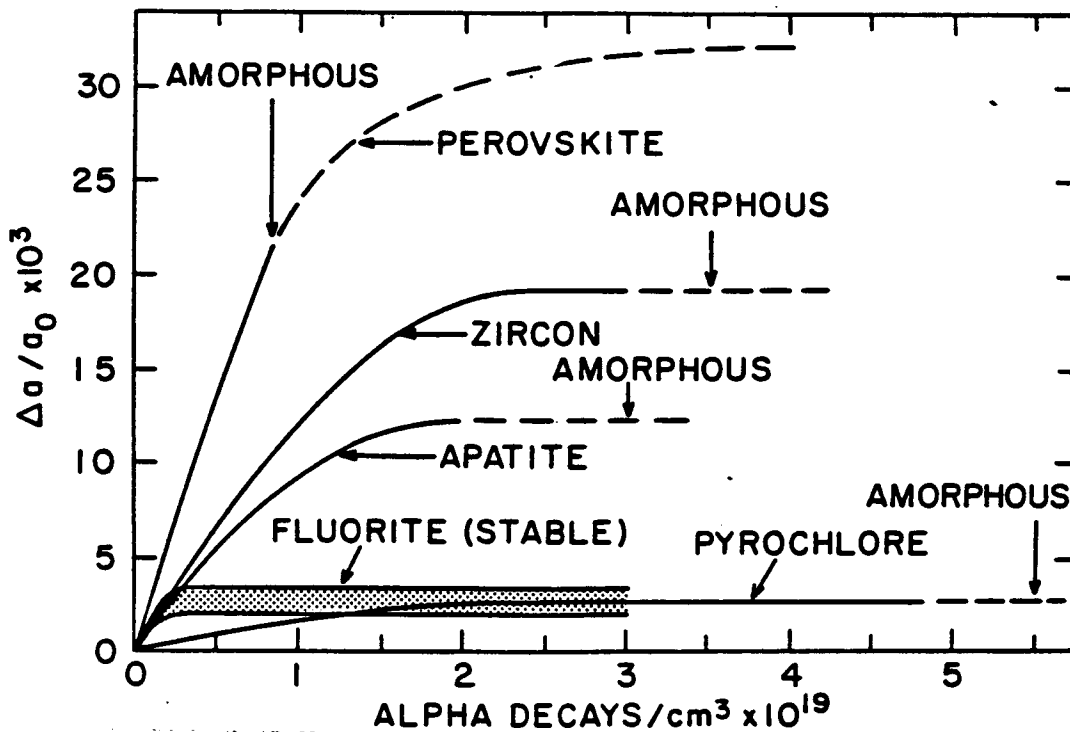


Figure 2. Lattice expansions as a function of internal alpha-recoil dose. Note the volume expansion is approximately three times the lattice expansion.⁵

Most studies of radiation damage in candidate waste forms have focused on the displacement damage caused by alpha particles or recoil nuclei. Accordingly, these radiation experiments have been performed either by actinide doping, ion bombardment, or neutron irradiation. It has been known for some time, however, that ionizing radiation can also change the physical properties of glasses. Shelby⁷ has found that borosilicate glasses exhibit an irradiation induced volume compaction near room temperature which can be as much as 30 times greater than that observed in vitreous silica at the same gamma dose. Volume compactions approaching 1% were observed at 10^{10} rads (Figure 3), a radiation dose which is at least an order of magnitude lower than that anticipated in certain HLW glass.⁸

Irradiation Induced Microcracking

In the study of 77-260 glasses by Weber,² devitrification produced crystalline gadolinium-apatite and cubic titanate phases. Microcracking was observed in all slow-cooled samples receiving a dose over 5×10^{17} alpha/cm³ (Figure 4). The extent of the microcracking was strongly dependent on dose, local crystal size, and crystal density. The cracking saturated at about the dose level where X-ray amorphization of the crystalline phase is complete.

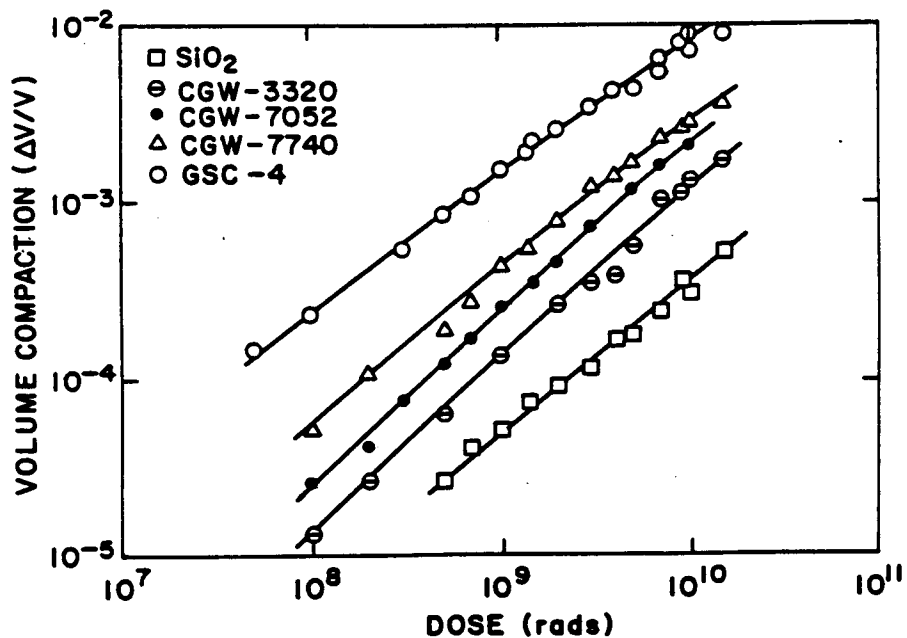
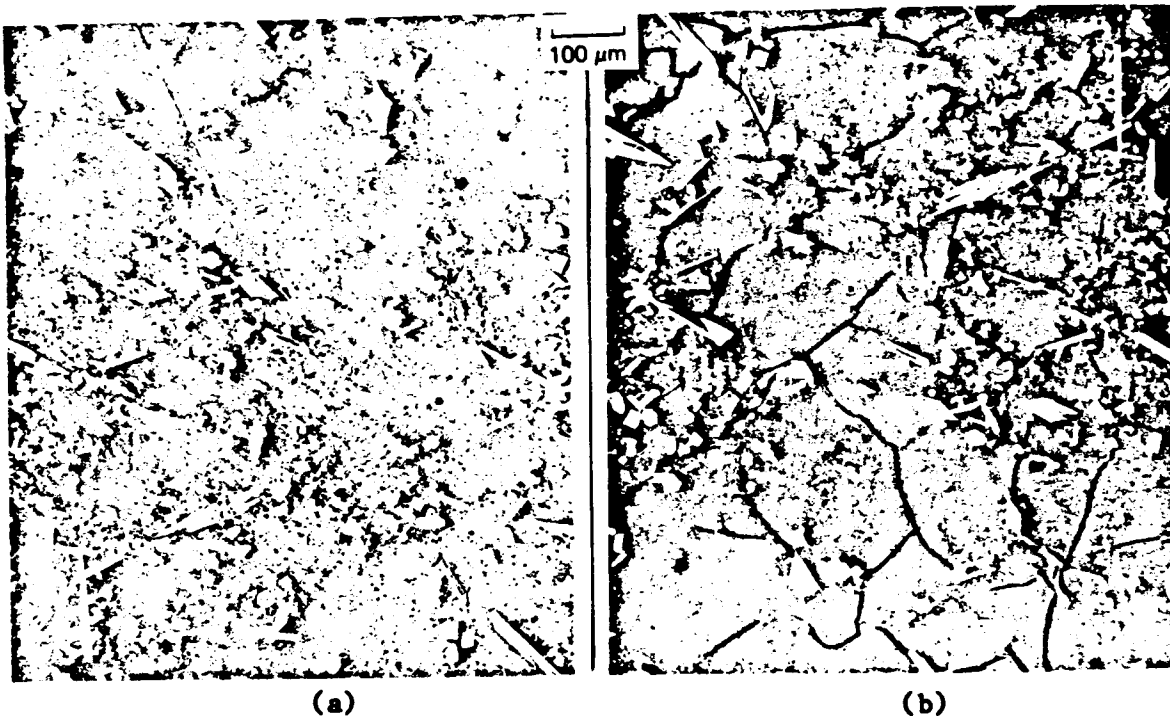


Figure 3. Effect of dose on the volume compaction of commercial borosilicate glasses.⁷



*Fig (b)
is upside
down
(same
area
micrograp*

Figure 4. Microstructure of the waste glass (77-260 glass) before and after microfracturing: (a) Slow cooled samples exhibiting no microcracks after 2×10^{16} decays/cm³; (b) Microcracks developed in same area after 8×10^{17} decays/cm³.²

Neutron irradiation also caused microcracking in synthetic barium hollandite (Figure 5) and perovskite, which are component phases of SYNROC, at a fluence considered equivalent to 2.2×10^{18} alpha/g.⁴ SYNROC B consisting of perovskite, hollandite and zirconolite showed much less severity in microcracking than that encountered in the individual phase studies.

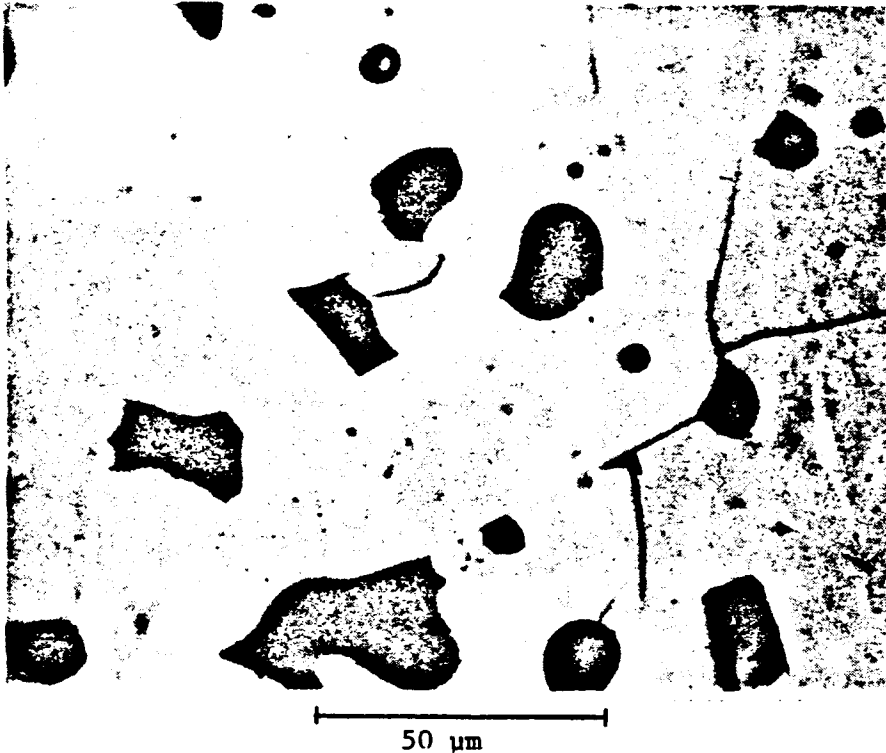


Figure 5. Appearance of hollandite after neutron irradiation.⁴

Estimation of Radiation Induced Stresses and Surface Area Increase

To understand the microcracking described above and to assess its consequences, we simplify the problem by assuming the volume changes in the waste form to be isotropic and elastic. First, we calculate the differential stress developed at the interface of a small spherical or cylindrical inclusion in a matrix. The inclusion represents a small crystalline particle in partially devitrified glass, a small grain or single phase domain in ceramic waste form, and a gas bubble. The differential stresses arise either from the difference in elastic moduli among phases (Case I), or from the difference in volume expansion among phases (Case II). We consider both effects independently. By comparing the calculated stresses to the strength of the glass and ceramics,

the nature of the microcracking is understood. Second, we estimate the total surface area increase due to microcracking by an energy balance method. We use a criterion from impact test,^{9,10} that 1% of the elastic strain energy is transformed to surface energy associated with the newly formed glass by cracking.

For the stress calculation, we employ the stress distribution in a sphere, in a shell, or a hollowed cylinder as determined from the linear isotropic elasticity theory. In the limit of infinite thickness of the shell or cylinder, the solution becomes the stress distribution in a matrix around a small inclusion or gas bubble imposed by a stress constraint from canister or backfill materials. By taking the stress at interface of the inclusion or gas bubble and the matrix, the maximum differential stresses are obtained. We have considered both the radial and tangential stresses. For the estimation of surface area increase, the elastic energy density is calculated upon the differential stress. By multiplying the volume of various sizes of existing canisters, the total energy stored is given. Dividing 1% of the total energy by the typical surface energy of glass and ceramics, the cracked surface area is obtained. The details of the above description are attached as an appendix.

Table 4 shows the calculated swelling pressure (σ) developed in glass and ceramic phases upon irradiation [Equation (3), Appendix].

Table 4. Pressure developed by 1% volume swelling. E = Young's modulus; ν = Poisson's ratio; σ = calculated pressure.

	Ceramic Phase [†]	Glass (Various Compositions)
E (MPa)	(6.9-41.4) $\times 10^4$	(4.8-6.9) $\times 10^4$
(psi)	(1.0-6.0) $\times 10^7$	(0.7-1.0) $\times 10^7$
ν	0.15-0.3	0.2-0.3
σ (MPa)	(4.1-34.5) $\times 10^2$	(2.8-5.6) $\times 10^2$
(psi)	(0.6-5.0) $\times 10^5$	(0.4-0.8) $\times 10^5$

[†]Data for alumina, zirconia and mullite

This table will be a basis for the calculation of differential stress and the cracked surface area described below. It should be emphasized that the pressure is calculated assuming no elastic or inelastic relaxation in surrounding constraints.

(I) Stress From the Difference of Elastic Moduli

We assume the same 1% volume expansion among phases; here the difference of the elastic moduli contributes the differential stress. The differential stress p (see Equations 1 and 2) is obtained by subtracting the stress in one phase by the stress in the other phase. The resulting stress at the interface of inclusions in glass or gas bubbles in glass or ceramic phase are shown in Table 5.

Table 5. The maximum stress of matrix at the interface of inclusions in glass or gas bubbles in glass or ceramic phase.

<u>Inclusion/Matrix</u>	<u>Maximum Stress</u>	
	<u>Glass</u>	<u>Ceramics</u>
Ceramics (MPa)	2.8×10^3	---
(psi)	4.0×10^5	
Gas Bubble (MPa)	1.2×10^3	-4.1×10^3
(psi)	1.8×10^5	-6.0×10^5

In the calculation, the pressure of gas generated has been varied from 0.10-10.13 MPa (1 to 100 atm) and the backfill stress has been taken as the fault stress of sandstone and lithographic limestone [i.e., $(2.4-3.3) \times 10^2$ MPa, $(3.5-4.8) \times 10^4$ psi].¹¹

For the stress generated from the anisotropy of ceramic phase, the anisotropy of elastic moduli among phases or grains has been varied from 1 to 10%. Table 6 shows the maximum stress developed by 1% and 10% difference in the elastic moduli.

Table 6. The maximum stress developed by 1% and 10% difference in elastic moduli in ceramic phase.

<u>Anisotropy (%) in Elastic Moduli</u>	<u>Maximum Stress</u>	
	<u>MPa</u>	<u>10^4 psi</u>
1	6.2×10^2	9
10	3.4×10^2	5

Considering the elastic moduli can change by an order of magnitude depending on the orientation in a single crystal, the 1 to 10% estimation is not unrealistically high in polycrystalline materials.

(II) Stress From the Differential Swelling Among Phases

In (I) we have simply assumed the differential stresses are from the difference of the elastic moduli. However, the volume expansion among phases may also be different as shown in Tables 2 and 3 and in Figure 5. This is either from the difference of inherent radiation susceptibility among phases or from the enrichment of radioactive isotopes in one phase as shown by Weber². We again assume a conservative 1% differential volume expansion (see Tables 2, 3, and Figure 5) at constant elastic moduli of ceramic phases, the maximum stress is obtained as shown in Table 7.

Table 7. Maximum stress of matrix at the interface of inclusions in glass and ceramics due to differential expansion.

Waste Forms	Maximum Stress	
	MPa	10 ⁵ psi
glass or ceramics	3.4x10 ³	5

Now we compare the calculated stress to the typical mechanical properties of selected ceramics and glasses listed in Table 8.

Table 8. Typical mechanical properties of selected ceramics and glasses.

	Compressive Strength		Tensile Strength		Reference
	MPa	(psi)	MPa	(psi)	
Alumina	up to 3.8×10^3	(5.5×10^5)	3.1×10^2	(4.5×10^4)	(12)
Zirconia	up to 1.3×10^3	(1.9×10^5)	1.4×10^2	(2.1×10^4)	(12)
Mullite	up to 1.3×10^2	(1.9×10^4)	1.1×10^2	(1.6×10^4)	(12)
Glass ⁺	9.0×10^3	(1.3×10^5)	6.9×10	(1.0×10^4)	(13)
Waste glass ⁺⁺	3.9×10	(5.7×10^3)			(9)

⁺ Glass composition has not been specified.

⁺⁺ Tensile or compression has not been specified.

Note the stresses of Tables 6 and 7 are large enough to fracture the glass, especially the waste glass. Also, since they are comparable to the strength of the ceramic phase, the ceramic matrix may also fracture in part. Further, the stress arises both from modulus difference and the differential swelling simultaneously. Real stresses, therefore, may be higher than the estimation in Tables 5-7.

Stress Relaxation

The quoted short-term laboratory experiments have been performed in an accelerated condition compared to the environment presumably existing in a HLW package. This fact cannot be overlooked in the glassy waste form for the present assessment since the glass is known to relax simultaneously with the stress generation described above. To correctly assess the radiation induced

cracking behavior in geologic time with the dose rate existing in a real HLW package, we adopt a zeroth order approximation of the relation of volume expansion to dose rate and relaxation time which has been recently developed by Martin²⁰ for gamma irradiated borosilicate glass.

$$\Delta V/V = KD (1 - \exp(-t/\zeta))$$

where K is the dilatation per unit dose, D the dose rate, ζ the relaxation time, and t the experiment time. Using this equation, we estimate the fractional decrease of ($\Delta V/V$) and the concomitant stress decrease.

Table 9 shows the radiation condition¹⁷ in the HLW package environment, and Table 10 indicates the dose rate used in the laboratory test.

Table 9. Radiation conditions in the HLW package environment.

<u>Radiation</u>	<u>Total Radiation</u>	<u>Duration</u>	<u>Dose Rate</u>
alpha	10^{18} α/g	10^{2-3} years	$3 \times 10^{7-8}$ $\alpha/(g-s)$
	10^{19} α/g	10^6 years	3×10^5 $\alpha/(g-s)$
beta, gamma	10^{12} rad	10^2 years	3×10^2 rad/s

✓
✓
✓
✓

Table 10. Dose rate used in the laboratory test.

<u>Source</u>	<u>Radiation</u>	<u>Dose Rate</u>
PNL ²	alpha	3×10^{10} $\alpha/(g-s)$
Shelby ⁵	gamma	2.3×10^3 rad/s

✓

As can be seen in the above tables, the alpha test has an acceleration factor of 10^2-10^3 , while the gamma test has a factor of 10 for the first 1000 years

in a repository. With the relaxation time obtained by Martin²⁰ from Shelby's data ($\tau=2$ years at 200°C), the ratios of $(\Delta V/V)$ in the waste environment to $(\Delta V/V)$ in the accelerated condition are obtained: For alpha, the ratio ranges from 2×10^{-2} to 2×10^{-3} , while it is 0.2 for gamma. These factors, in effect, will reduce the stress generated in the amount of these ratios. In spite of this reduction factor, the reduced stresses are still comparable to the fracture strength of waste glass (refer to Tables 5, 7 and 8).

The relaxation time for alpha damage in glass and the relaxation behavior in ceramic phases are not known at the present time. The relaxation in ceramics is speculated to be slower than the glassy phases. Also, the contribution of alpha and gamma rays are taking place simultaneously. Therefore, the above assessment of relaxation after gamma irradiation upon glass may be conservative in a real HLW package; concomitantly the radiation induced cracking is considered to be a potentially important detrimental factor to waste form integrity in the geologic time.

Effects of Cracks on Surface Area and Leaching

Using the 1% differential volume expansion at fixed elastic moduli, the ratio of the surface area after cracking to the initial surface area ranges to maximum 50 for glass and 30 for ceramics for various sizes of the existing canister.^{9,14,17} The surface energy used was 300 erg/cm² for glass and 1000 erg/cm² for ceramics.

In the early study of ^{244}Cm doped and devitrified 77-260 waste glass,² it appeared that microfracturing has no measurable effect on the net material leached. However, since the localized radiolysis effect at the sample-solution interface could have masked the effects of structural changes, it is difficult to pull out the cracking effect separately from this study.

Recently, more systematic simulation has been performed by Perez, et al.²¹ Cracks have been simulated by stacking glass pellets and platinum wire spacers and then holding them together with a stainless clamp. They have found that crack depth and crack width are important parameters in the release from cracks and that there may be a minimum crack depth before leaching from the cracks become important. More than factor two enhancement of leach rate has been observed in the simulated cracked sample compared to glass monolith as shown in Figure 6 where solid cylinder represents the monolith while pellets are simulated cracked samples. It has also been found that the leach rates from the crack surfaces are two to three times lower than the leach rates of the outer exposed surfaces. Considering our estimation of the surface area, increase is much higher than that of the present experiment, it is possible that the leach rates are significantly affected by the radiation induced microcracking in geologic time. More quantitative assessment is premature at the moment with the lack of a detailed experimental basis.

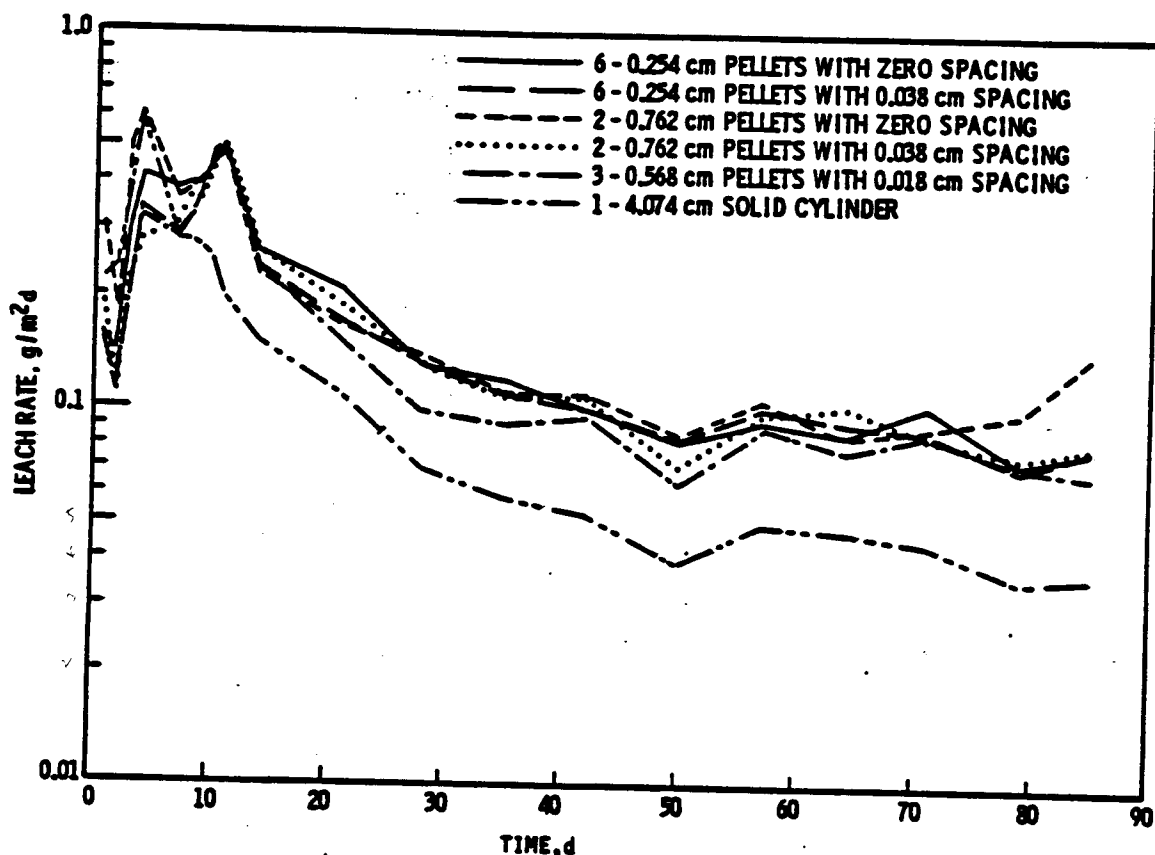


Figure 6. Leach rate (g-glass/m²d) based on silicon vs time for 1.90-cm-diameter pellets.¹⁸

Further Implications

As described in the attached appendix, we estimated the stress generated at the interfaces of particles in metal matrices, coated particles and molecular stuffed glass, and at the canister (Case III). In these cases, the thickness of the shell and the cylinder is finite and the net stress p is sim-

ply a swelling pressure of the radionuclide loaded waste form, since the displacement damage in coating, cladding material, or canister is negligible compared to that in the loaded waste. The calculated results are not presented here since the available experimental data are meager, except for HTGR (High Temperature Gas-Cooled Reactor) coated particles. Rather, we simply describe the possible consequences from this calculation associated with the differential swelling analogous to the assessment of partially devitrified glass and ceramics.

- With the radiation induced stress at the interfaces of particles in metal matrices, the glass particles and a part of the ceramic particles may crack. Likewise, the coatings (Al_2O_3 , PyC or glass) may experience cracking unless a properly engineered design reduces the stress, such as using a microporous carbon coating before the main coating as in HTGR fuel. Also, the cladding and the core regions of the molecular stuffed glass may reveal similar cracking. This cracking may enhance the radioactive isotope leachability.
- Upon swelling of the waste form, most metal containers may experience imposed stress. The stress may lead to the yielding of most canister materials. The residual stresses stored by plastic deformations of canisters will be a detrimental factor which could result in stress corrosion cracking and hydrogen embrittlement, leading to a breakage of the canisters in a repository condition.

Summary and Conclusions

Our first-order calculation indicates that radiation induced stresses might cause microfracturing in the radionuclide host phase of certain crystalline and glassy waste forms. This finding is in qualitative agreement with recent experimental results. Further, the calculation suggests that microfracture could increase surface area to a point where leaching behavior is significantly affected.

In certain multi-barrier systems, substantial stresses are calculated for inert layers or containers which constrain the RN host phase. If uncompensated for, these stresses might cause premature barrier failure or reduce durability. Here only little relevant experimental data is presently available; experience with HTGR particles indicates that such stresses may be effectively reduced either by the use of porous intermediate layers, or RN host phases which are not fully dense.

The scoping calculation contains a number of uncertainties and simplifying assumptions; quantitative estimates may be conservative, and must be considered subject to confirmation. We believe, however, that in view of the present results, the possible effects of radiation induced stresses should receive explicit consideration in waste package designs.

References

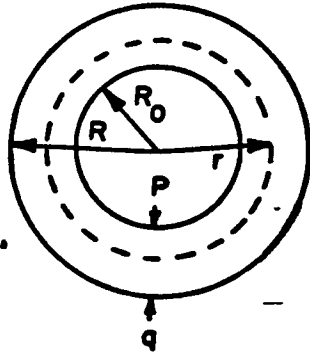
1. J. E. Mendel, et al., Annual Report on the Characterization of High Level Waste Glass, PNL Report, BNWL-2252, June, 1977.
2. W. J. Weber, et al., "Radiation Effects in Vitreous and Devitrified Simulated Waste Glass," p. 294 in Ceramics in Nuclear Waste Management, U.S. DOE Conference Proceedings, CONF-790420, May 1979.
3. R. Dayal, K. J. Swyler, and P. Soo, NRC Nuclear Waste Management Technical Support in the Development of Nuclear Waste Form Criteria. Task 1: Waste Package Overview, BNL Informal Report, BNL-NUREG-27961, June 1980.
4. K. D. Reeve and J. L. Woolfrey, "Accelerated Irradiation Testing of SYNROC Using Fast Neutrons - I. First Results on Barium Hollandite, Perovskite and Undoped SYNROC B," J. Austr. Ceram. Soc. 16, May (1980).
5. W. J. Weber, J. W. Wald, and W. J. Gray, Radiation Effects in Crystalline High Level Waste Nuclear Waste Solid, PNL Report, PNL-SA-8732, 1980.
6. J. M. Rusin, W. J. Gray, and J. W. Wald, Multibarrier Waste Form Part II: Characterization and Evaluation, PNL Report, PNL-2668-2, 1979.
7. J. Shelby, J. Appl. Phys. 51(5), 2561 (1980); 50(5), 3702 (1979).

8. K. S. Czyscinski, K. J. Swyler, and C. J. Klamut, NRC Nuclear Waste Management Technical Support in the Development of Nuclear Waste Form Criteria, BNL Informal Report, BNL-NUREG-27773, 1980.
9. S. C. Slate, et al., Stresses and Cracking in HLW Glass, PNL Report, PNL-SA-7369, 1978.
10. W. J. Mecham, et al., "Characterization of Impact Fracture of Brittle Solid Waste Forms," in Proceedings of the Materials Research Society Meeting, Boston, 1979.
11. F. A. Donath, "Relation of Solids to Nuclear Waste Isolation," in Proceedings of the Conference on High Level Radioactive Solid Waste Forms, Denver, 1978, p. 13.
12. Handbook of Materials Science, CRC, Vol. I-III, 1975.
13. F. A. McClintock and A. S. Argon, Mechanical Behavior of Materials, Addison-Wesley Co., 1966.
14. J. M. Rusin, M. F. Browning, and G. J. McCarthy, "Development of Multibarrier Nuclear Waste Forms," in Scientific Basis for Nuclear Waste Management, Vol. 1, Edited by G. J. McCarthy, Plenum Press, 1978, p. 169.
15. T. H. Smith, et al., Impact Testing of Vitreous Simulated HLW in Canisters, PNL Report, BNWL-1903, 1975.

16. J. W. Braithwaite and M. A. Molecke, "HLW Canister Corrosion Studies Pertinent to Geologic Isolation," p. 243, *ibid.* Reference 11.
17. P. E. Ahlström, "Ceramic and Pure Metal Canisters in Buffer Material," p. 283, *ibid.* Reference 11.
18. E. B. Shand, Glass Engineering Handbook, McGraw-Hill, 1958, p. 24.
19. W. D. Kingery, Introduction to Ceramics, John Wiley and Sons, Inc., New York, 1967, p. 194.
20. D. M. Martin, Thermal Stresses in Waste Disposal Systems, Iowa State University Report prepared for SAFER Division, Office of Nuclear Regulatory Research, U. S. Nuclear Regulatory Commission, September 1980.
21. J. M. Perez, Jr. and J. H. Westik, Jr., "Effects of Cracks on Glass Leaching," in abstracts of ORNL Conference on the Leachability of Radioactive Solids, Gatlinburg, December 1980.
22. S. G. Lekhnitskii, Theory of Elasticity of an Isotropic Elastic Body, Holden-Day Series in Mathematical Physics, 1963, p. 358, p. 390.

APPENDIX

Consider a sphere in a shell (3 dimensions) or a filled cylinder (2 dimensions) as shown in Figure A.1, where R_0 and R are the inner and outer radii, and (r, θ, ϕ) is a spherical coordinate while (r, θ, z) is a cylindrical coordinate. P and q are the inner and outer pressure, respectively. The spherical coordinate is pertinent to an inclusion in matrix and to particles in metal matrix while the cylindrical coordinate is used in the calculation of the stresses of the canister.



R_0 : inner diameter
 R : outer diameter
 P : inner pressure
 q : outer pressure

Figure A.1. Schematic of an isotropic spherical inclusion of a hollowed cylinder.

In the spherical coordinate, the stress distribution is:(21)

$$\sigma_r = \frac{PR_0^3 - qR^3}{R^3 - R_0^3} + \frac{(q-P)R_0^3 R^3}{R^3 - R_0^3} \frac{1}{r^3} \quad (1)$$

$$\sigma_\phi = \sigma_\theta = \frac{PR_0^3 - qR^3}{R^3 - R_0^3} - \frac{(q-p)R_0^3 R^3}{R^3 - R_0^3} \frac{1}{r^3}$$

And in the cylindrical coordinate,

$$\begin{aligned}\sigma_r &= - \frac{qR^3 - PR_o^3}{R^2 - R_o^2} + \frac{(q-P)R^2 R_o^2}{R^2 - R_o^2} \frac{1}{r^2} \\ \sigma_\theta &= - \frac{qR^2 - PR_o^2}{R^2 - R_o^2} - \frac{(q-P)R^2 R_o^2}{R^2 - R_o^2} \frac{1}{r^2} \\ \sigma_z &= 0\end{aligned}\tag{2}$$

To proceed further, one must determine the pressures p and q . The pressure (or stress) q is simply that imposed by external constraints; for the present case we take this as being due to the backfill or host rock material around an emplaced waste package. The internal pressure p requires more detailed consideration. We are unaware of any direct measurements of the pressure which is exerted when waste form materials are irradiated in constrained volumes. One can imagine two limiting cases: (A) The external constraints effectively prohibit any significant expansion or compaction of the waste form material. (B) The material expands or compacts to a degree which is sensibly that which is measured under unconstrained conditions. Almost certainly, the actual situation is an intermediate between these two cases; the equilibrium pressure p may depend sensitively on the degree of expansion or compaction which has occurred. However, in the absence of relevant experimental data, we have chosen to consider the "static" case (A): The pressure p is chosen as that which is required to reverse given irradiation induced volume changes in the waste form material. As mentioned, this prescription provides for no elastic relaxation, and quite possibly over estimates maximum stresses. It

has the advantage, however, of producing results which are independent of scale, since a detailed analysis of strains is not required; moreover, estimates are at least conservative. Adopting this prescription, and assuming isotropic volume changes, the stress (or pressure) developed upon swelling is given by¹³:

$$\sigma = \frac{E}{(1 - 2\nu)} \frac{\Delta V}{3V} \quad (3)$$

where, $(\Delta V/V)$ represents volume expansion, E Young's modulus, and ν Poisson's ratio.

The differential stress p is obtained by subtracting the stress σ of one phase from the stress σ of the other phase, if required.

Inclusions are very small compared to the canister. Also, confining ourselves to the interface of the inclusion and matrix,

$$\begin{aligned} \sigma_r &= -p \\ \sigma_\theta &= \sigma_\theta = -2q + p \end{aligned}$$

by the simplification of Equations (1) and (2) with

$$\begin{aligned} r &\rightarrow R_0 \\ R/R_0 &\rightarrow \infty \end{aligned}$$

We extend our consideration to several other cases presumably taking place in an HLW package. Equations (1) and (2) are equally applicable here also as described below:

Particles in Metal Matrix

At the interface of the small particles in the matrix, Equation (4) is used. Here p represents the swelling pressure of the particles [Equation (3)] and of the yield stress of the metal matrix.

Coated Particles in Metal Matrix

Equation (1) is used considering the stresses in the middle of coating [$r = (R+R_0)/2$], where p represents the swelling pressure of the particles [Equation (3)], q the yield stress of the metal matrix, R_0 the radius of the particles, and $(R-R_0)$ the thickness of the coating.

Molecular Stuffed Glass

Equation (2) is used. P represents the swelling pressure of the core region while q the yield stress of the metal canister. The thickness of the cladding is $(R-R_0)$.

Stresses in Canister

Equation (2) is used for a cylindrical canister. R_0 represents the radius of the waste form, $(R-R_0)$ the thickness of the canister, P the swelling pressure of the whole waste form [Equation (3)], and q the stress constraint imposed by overpack. We confine the calculation to the stress at $r = (R+R_0)/2$.

The positive signs of the stresses follow the direction shown in Figure 7, while the negative signs are for the opposite direction. Also, the bigger was chosen between radial stress and tangential stress.

For the calculation of the cracked surface area, the elastic strain energy per unit volume stored upon swelling, ϵ , is used:

$$\epsilon = \frac{E}{2(1 - 2\nu)} \left(\frac{\Delta V}{3V}\right)^2$$

The cracked surface areas, s , are obtained by:

$$s = \frac{0.01 \times \epsilon \times \text{canister volume}}{\text{surface energy of waste form}}$$